Quantum information processing and multiplexing with trapped ions

D. J. Wineland[1], D. Leibfried[1], B. DeMarco[1], V. Meyer[1], M. Rowe[2], A. Ben-Kish[3], M. Barrett[1], J. Britton[1], J. Hughes[4], W. M. Itano[1], B. M. Jelenković[5], C. Langer[1], D. Lucas[6], and T. Rosenband[1]

[1] *Time and Frequency Division, NIST, Boulder*

[2] *current address: Optoelectronics Division, NIST, Boulder*

[3] *current address: Department of Physics, Technion, Haifa, Israel*

[4] *current address: Department of Physics, University of Virginia*

[5] *Institute of Physics, Belgrade, Yugoslavia*

[6] *current address: Department of Physics, Oxford University, U.K.*

Abstract

We report experiments on coherent quantum-state synthesis and control of trapped atomic ions. This work has the overall goal of performing large-scale quantum information processing; however, such techniques can also be applied to fundamental tests and demonstrations of quantum mechanical principles, as well as to the improvement of quantum-limited measurements.

1 Introduction

Efforts to realize experimentally the elements of quantum computation (QC) by use of trapped atomic ions have been stimulated in large part by a 1995 paper by Cirac and Zoller [1]. In this scheme, ions confined in a linear RF (Paul) trap are cooled and form a stable spatial array whose motion is described by normal modes. Two internal levels in each ion form a qubit (referred to as a spin qubit below). Typically, the spacing between ions ($> 1\ \mu m$) is large enough that the direct coupling of internal states of two ions is negligible, thereby precluding logic gates based on internal-state interactions.[1] Cirac and Zoller [1] suggested cooling the ions to their motional ground state and using the ground and first excited state of a particular motional mode as a qubit (motion qubit). The motional mode can act as a data bus to transfer information between ions by first mapping the spin qubit state of a particular ion onto the selected motion qubit by use of a laser beam focused onto that ion. Being able to perform logic gates between the motion qubit and another selected spin qubit, coupled with the ability to perform single spin qubit rotations provides the basis for universal quantum computation [3, 4].

The ion-trap scheme satisfies the main requirements for a quantum computer as outlined by DiVincenzo [5]: (1) a scalable system of well-defined qubits, (2) a method to reliably initialize the quantum system, (3) long coherence times, (4) existence of universal gates, and (5) an efficient measurement scheme. Most of these requirements have been demonstrated experimentally; consequently, ion-trap quantum processors are studied in several laboratories. Here, we focus on experiments carried out at NIST but note that similar work is being pursued at Aarhus, Almaden (IBM), Hamburg,

[1] "Dipole blockade" gates [2] based on Rydberg states as envisioned for neutral atoms are a possibility, but these gates are experimentally more challenging for ions because of the higher energies between ground and Rydberg levels.

Hamilton (Ontario, McMaster Univ.), Innsbruck, Los Alamos (LANL), University of Michigan, Garching (MPI), Oxford, and Teddington (National Physical Laboratory, U.K.). For brevity, we discuss only recent work on logic gates and steps towards scaling to a large system.

2 Coherent quantum control

The key entangling operation in the Cirac/Zoller scheme for QC, and the key to quantum gates between ions, is an operation that couples a spin qubit with the selected motion qubit. Assume that the spin qubit has a ground state (labeled $|\downarrow\rangle$) and a higher metastable state (labeled $|\uparrow\rangle$) that are separated in energy by $\hbar\omega_0$. Assume transitions between these levels can be excited with a focused laser beam. The interaction between an ion and the electric field of the laser beam can be written as

$$H_I(t) = -\widetilde{d}E = -\widetilde{d}E_0\cos(k\widetilde{z} - \omega_L t + \phi), \tag{1}$$

where $\widetilde{d}$ is the electric dipole operator, $\widetilde{z}$ is the ion position operator for displacements from the ion's equilibrium position (expanded in terms of normal mode operators), k is the laser beam's k-vector (taken to be parallel to $\hat{z}$), ω_L is the laser frequency, and ϕ is the phase of the laser field at the mean position of the ion. E is the laser's electric field, which is assumed to be classical. The dipole operator $\widetilde{d}$ is proportional to $\sigma^+ + \sigma^-$, where $\sigma^+ \equiv |\uparrow\rangle\langle\downarrow|, \sigma^- \equiv |\downarrow\rangle\langle\uparrow|$, and we take $\widetilde{z} = z_0(a + a^\dagger)$, where a and $a^\dagger$ are the lowering and raising operators for the harmonic oscillator of the selected motional mode (frequency ω_z) and $z_0 \equiv \sqrt{\hbar/2m\omega_z}$ is the extension of the ground-state wavefunction. (Here, we assume all other z modes are cooled to and remain in their ground states, and for simplicity have neglected them in $\widetilde{z}$.) In the Lamb-Dicke limit, where the extent of the ion's motion is much less than $\lambda/2\pi = 1/k$, we can write Eq. (1) (in the interaction frame, and making the rotating wave approximation [6]) as

$$H_I(t) \simeq \hbar\Omega\sigma^+ e^{-i(\omega_L-\omega_0)t+\phi}[1 + i\eta(ae^{-i\omega_z t} + a^\dagger e^{i\omega_z t})] + h.c.\,. \tag{2}$$

Here, $\Omega \equiv E_0 d_{\downarrow\uparrow}/(2\hbar)$ where $d_{\downarrow\uparrow}$ is the electric-dipole matrix element between $|\downarrow\rangle$ and $|\uparrow\rangle$ and $\eta = kz_0$ is the Lamb-Dicke parameter ($\ll 1$ in the Lamb-Dicke limit).

For certain choices of ω_L, H_I is resonant and the spin and motion can be coupled efficiently. For example, when $\omega_L = \omega_0 - \omega_z, H_I \simeq i\eta\hbar\Omega\sigma^+ a e^{i\phi} + h.c.$. This is usually called the "red-sideband" coupling and is formally equivalent to the Jaynes-Cummings Hamiltonian [7] from quantum optics. Here, $|\downarrow\rangle \rightarrow |\uparrow\rangle$ transitions are accompanied by $|n\rangle \rightarrow |n-1\rangle$ motional mode transitions. When $\omega_L = \omega_0 + \omega_z, H_I \simeq i\eta\hbar\Omega\sigma^+ a^\dagger e^{i\phi} + h.c.$, the "blue sideband," and $|\downarrow\rangle \rightarrow |\uparrow\rangle$ transitions are accompanied by $|n\rangle \rightarrow |n+1\rangle$ transitions. When $\omega_L = \omega_0$, $H_I \simeq \hbar\Omega\sigma^+ e^{i\phi} + h.c.$ and $|\downarrow\rangle \rightarrow |\uparrow\rangle$ transitions do not change n. These "carrier" transitions are used to perform the single spin-qubit rotations.

In the $^9Be^+$ experiments at NIST, two laser beams are used to drive two-photon stimulated-Raman transitions between two ground-state hyperfine spin-qubit levels ($|\downarrow\rangle \equiv |F=2, m_F=-2\rangle$; $|\uparrow\rangle \equiv |F=1, m_F=-1\rangle$). Here, k must be replaced by the difference Δk between k-vectors for the two Raman beams, ϕ is replaced by the phase difference between the laser beams, and $\Omega \propto E_1 E_2/\Delta$, where $E_{1,2}$ are the electric fields of the two beams and Δ is the nominal detuning of the beams from an allowed transition [6]. When the difference frequency of the Raman beams is tuned to

resonance with the red or blue sidebands, entanglement between the ion and motion qubit occurs according to the coherent evolution

$$|\downarrow\rangle|n\rangle \rightarrow cos(\Omega_{n,n'}t)|\downarrow\rangle|n\rangle - ie^{i\phi}sin(\Omega_{n,n'}t)|\uparrow\rangle|n'\rangle \quad (3)$$

and

$$|\uparrow\rangle|n\rangle \rightarrow -ie^{-i\phi}sin(\Omega_{n,n'}t)|\downarrow\rangle|n\rangle + cos(\Omega_{n,n'}t)|\uparrow\rangle|n'\rangle. \quad (4)$$

Here, $n' = n \pm 1$ and $\Omega_{n,n'} \equiv \eta\Omega(n_>)^{1/2}$, where $n_>$ is the greater of n or n'. For each ion we are free to choose $\phi = 0$ but the phase of all operations on this ion must be referenced to this choice.[2] Carrier transitions can also be described by expressions (3) and (4) where $n = n'$ and $\Omega_{n,n} = \Omega$. Since η must be kept large enough that the time to carry out an entangling operation is not too long, our interaction does not rigorously satisfy the Lamb-Dicke criterion. Therefore, we must add corrections to the expressions for the Rabi frequencies $\Omega_{n,n'}$. These correction factors, which can be called Debye-Waller factors [6], have been observed [8] and form the basis for a controlled-not (CNOT) gate described below.

To initialize the qubits for each experiment, we use a combination of internal-state optical pumping (to pump to the $|\downarrow\rangle$ state) and sideband laser cooling to optically pump the motional modes to their ground states [9] - [12]. As in many atomic physics experiments, the observable in the ion-trap experiments is the ion's spin qubit state. We can efficiently distinguish $|\downarrow\rangle$ from $|\uparrow\rangle$ using a cycling transition to implement "quantum jump" detection [13].

3 Gates

Equations (3) and (4) illustrate the basic source of entanglement in ion experiments from which universal logic gates have been constructed. For example, a CNOT and π-phase gate between the motion and spin qubit for a single ion have been realized at NIST [6, 14]. Also, using the scheme suggested by Sørensen and Mølmer [15, 16] and Solano *et al.* [17], the NIST group realized a universal gate between two spin qubits [18, 19]. Compared to the original Cirac and Zoller gate [1], this last gate has the advantages that (1) laser-beam focusing (for individual ion addressing) is not required, (2) it can be carried out in one step, (3) it does not require use of an additional internal state, and (4) it does not require precise control of the motional state (as long as the Lamb-Dicke limit is satisfied). From this gate, a CNOT gate can be constructed [15]. In recent experiments, we have significantly reduced motional heating [20] allowing us to explore new types of gates and improve the fidelity of the operations.

3.1 Controlled-NOT wave-packet gate

Recently, we have demonstrated experimentally [21] a new kind of CNOT gate between the motion qubit (control bit) and spin qubit (target bit) that was proposed in Ref. [22]. This gate uses carrier transitions and relies on Debye-Waller correction factors to provide the conditional dynamics for the gate. Including these correction factors

[2] In general, the laser phases (mod 2π) are not the same on each ion so the effective Bloch vectors for each ion are oriented differently in the lab frame. The choice $\phi = 0$ for each ion means that the spin coordinate frame for each ion is different.

[6], the n-dependent carrier Rabi frequencies become:

$$\Omega_{n,n} = \Omega e^{-\eta^2/2} L_n(\eta^2), \tag{5}$$

where $L_n(X)$ is the Laguerre polynomial of order n. For the lowest three values of n, we have

$$L_0(\eta^2) = 1, \quad L_1(\eta^2) = 1 - \eta^2, \quad L_2 = 1 - 2\eta^2 + \eta^4/2. \tag{6}$$

To construct the CNOT gate we could, for example, configure the experiment to make $\eta^2 = 1/2$ and drive the carrier transition for a time such that $\Omega_{0,0}t = \pi$ [22]. We find the state transformations (choosing $\phi = 0$) $|\downarrow\rangle|0\rangle \rightarrow -|\downarrow\rangle|0\rangle$, $|\uparrow\rangle|0\rangle \rightarrow -|\uparrow\rangle|0\rangle$, $|\downarrow\rangle|1\rangle \rightarrow -i|\uparrow\rangle|1\rangle$, and $|\uparrow\rangle|1\rangle \rightarrow -i|\downarrow\rangle|1\rangle$. Up to phase factors that can be corrected by single-ion qubit rotations (or accounted for in software[3]), this gate is the CNOT gate: if the control bit is a 1, the spin qubit flips, if the control bit is a 0, the spin qubit remains unchanged. In the experiment, the single-ion oscillation frequency and Lamb-Dicke parameter η are related by $\omega_z/2\pi(\text{MHz}) = 0.453/\eta^2$, so to carry out the gate we want $\omega_z/2\pi = 0.906$ MHz. Because the ion heating was fairly strong at this relatively low frequency, we chose $\eta^2 = 0.129$ which gave $\omega_z/2\pi = 3.51$ MHz and relatively small heating. For the motional qubit states we chose $|n = 0\rangle$ and $|n = 2\rangle$ so that the chosen value of η gave $\Omega_{0,0}/\Omega_{2,2} = 4/3$. Therefore, by choosing the interaction time such that $\Omega_{0,0}t = 2\pi$, we also realize the desired CNOT gate. Compared to the previously realized CNOT gate between motion and spin [14] this gate has the advantages that (1) it requires one step instead of three, (2) it does not require an auxiliary internal state, and (3) it is immune to Stark shifts caused by coupling to "spectator" states [6] (here, Stark shifts from coupling to non-resonant sideband transitions). This gate is fundamentally different from previously demonstrated gates in that it relies on the wave-packet nature of the ions. To obtain the correct interaction with the laser, we must average the laser field over the extent of the ion's wave packet rather than assuming it is a point particle.

3.2 Geometrical phase gate between two ions

In a separate experiment, we realized a (π) phase gate between two spin qubits [23] that carried out the state transformations: $|\downarrow\rangle|\downarrow\rangle \rightarrow |\downarrow\rangle|\downarrow\rangle$, $|\downarrow\rangle|\uparrow\rangle \rightarrow |\downarrow\rangle|\uparrow\rangle$, $|\uparrow\rangle|\downarrow\rangle \rightarrow |\uparrow\rangle|\downarrow\rangle$, and $|\uparrow\rangle|\uparrow\rangle \rightarrow -|\uparrow\rangle|\uparrow\rangle$. Combined with single bit rotations, it yields the CNOT operation. The gate relies in part on properties of motional states as they are displaced in phase space. For a particular motional mode, the displacement operator can be written [24]

$$D(\alpha) = e^{\alpha a^\dagger + \alpha^* a}, \tag{7}$$

where α is a complex number. For two successive displacements we have

$$D(\alpha)D(\beta) = D(\alpha + \beta)e^{iIm[\alpha\beta^*]}. \tag{8}$$

Now consider constructing a closed path in phase space so that the state returns to its original position. We can derive the effects of this transformation by constructing the closed path from a series of successive applications of Eq. (8) with infinitesimal

[3]Neglecting the overall minus sign, the transformation looks like the desired CNOT operation followed by a $\pi/2$ phase shift ($i = e^{i\pi/2}$) on the $|1\rangle$ state of the motion qubit. This phase shift can be removed by shifting the phase of the relevant laser oscillator for the next operation on the motion qubit.

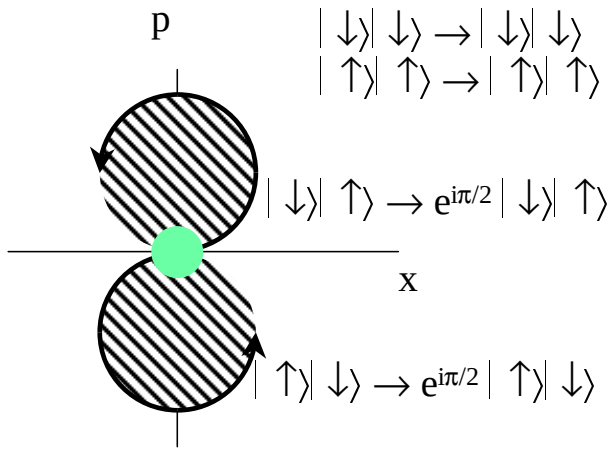

Figure 1: Schematic representation of the displacements of the axial stretch-mode amplitude in phase space for the four basis states of the two spin qubits. The detuning and amplitude of the displacements are chosen to give a $\pi/2$ phase shift on the $|\downarrow\rangle|\uparrow\rangle$ and $|\uparrow\rangle|\downarrow\rangle$ states while the $|\downarrow\rangle|\downarrow\rangle$ and $|\uparrow\rangle|\uparrow\rangle$ states are unaffected because the optical dipole forces for these states do not couple to the stretch mode.

displacements. The net effect is that the mode wavefunction acquires an overall phase shift that depends on the area enclosed by the path.

The second element required for the gate is to make the path area be spin dependent. This is accomplished by making the displacement in phase space with a spin-dependent optical dipole force as was done in previous experiments [25, 26]. To implement this gate on two ions, the Raman transition beams were separated in frequency by $\sqrt{3}\omega_z + \delta$, where $\sqrt{3}\omega_z$ is the stretch-mode frequency for two ions and δ is a small detuning (below). The separation of the ions was adjusted to be an integer multiple of $2\pi/\Delta k$ so that the optical-dipole force (from the "walking" standing wave) on each ion was in the same direction if the ions were in the same spin state but, due to the choice of laser polarizations, in opposite directions if the spin states were different. This had the effect that the application of the laser beams to the $|\downarrow\rangle|\uparrow\rangle$ and $|\uparrow\rangle|\downarrow\rangle$ states caused excitation on the stretch mode but the $|\downarrow\rangle|\downarrow\rangle$ and $|\uparrow\rangle|\uparrow\rangle$ states were unaffected. The detuning δ and duration of the displacement pulses were chosen to make one complete (circular) path in phase space with an area that gave a phase shift of $\pi/2$ on the $|\downarrow\rangle|\uparrow\rangle$ and $|\uparrow\rangle|\downarrow\rangle$ states. Under these conditions, the overall transformation was: $|\downarrow\rangle|\downarrow\rangle \rightarrow |\downarrow\rangle|\downarrow\rangle$, $|\downarrow\rangle|\uparrow\rangle \rightarrow e^{i\pi/2}|\downarrow\rangle|\uparrow\rangle$, $|\uparrow\rangle|\downarrow\rangle \rightarrow e^{i\pi/2}|\uparrow\rangle|\downarrow\rangle$, and $|\uparrow\rangle|\uparrow\rangle \rightarrow |\uparrow\rangle|\uparrow\rangle = e^{i\pi}e^{-i\pi}|\uparrow\rangle|\uparrow\rangle$. This is shown schematically in Fig. 1. Therefore, this operator acts like the product of an operator that applies a $\pi/2$ phase shift to the $|\uparrow\rangle$ state on each ion separately (a non-entangling gate) and a $-\pi$ phase gate. The effects of the first can be removed by single-ion qubit rotations (or accounted for in software) leaving the desired phase gate. The origin of this phase gate can also be viewed as a particular case of the more general formalism developed in Refs. [15], [27], and [28]. Compared to the original Cirac and Zoller gate [1], this shares the same advantages as the Sørensen and Mølmer [15, 16] gate realized in [18].

4 Whither quantum computation?

Although simple operations among a few ion qubits have been demonstrated, a viable quantum computer must look towards scaling to very large numbers of qubits. As the number of ions in a trap increases, several difficulties are encountered. For example, the addition of each ion adds three vibrational modes. It soon becomes nearly impossible to spectrally isolate the desired vibrational mode unless the speed of operations is slowed to undesirable levels [6, 29]. Furthermore, since error correction will most likely be incorporated into any large processor, it will be desirable to measure and reset ancilla qubits without disturbing the coherence of logical qubits. Since ion qubits are typically measured by means of state-dependent laser scattering, the scattered light from ancilla qubits held in a common trap may disturb the coherence of the logical qubits.

For these and other reasons, it appears that a scalable ion-trap system must incorporate arrays of interconnected traps, each holding a small number of ions. The information carriers between traps might be photons [30] - [32], or ions that are moved between traps in the array. In the latter case, a "head" ion held in a movable trap could carry the information by moving from site-to-site as in the proposal of Ref. [33]. Similarly, as has been proposed at NIST, we could shuttle ions around in an array of interconnected traps [6, 34]. In this last scheme, the idea is to move ions between nodes in the array by applying time-dependent potentials to "control" electrode segments. To perform logic operations between selected ions, these ions are transferred into an "accumulator" trap for the gate operation. Before the gate operation is performed, it may be necessary to sympathetically re-cool the qubit ions with another ion species [6]. Subsequently, these ions are moved to memory locations or other accumulators. This strategy always maintains a relatively small number of motional modes that must be considered and minimizes the problems of ion/laser-beam addressing using focused laser beams. Such arrays also enable highly parallel processing and ancilla qubit readout in a separate trapping region so that the logical ions are shielded from the scattered laser light.

4.1 "Dual" linear ion trap

We have implemented some of the the first steps towards realizing this scheme by moving ions in the "dual" trap shown in Fig. 2. The trap was constructed from a stack of metallized 200 μm thick alumina wafers. Laser-machined slots and gold traces created the desired electrode geometry [20]. Gold traces of 0.5 μm thickness were made with evaporated gold that was transmitted through a shadow mask and deposited on the alumina. Subsequently, an additional 3 μm of gold was electroplated onto the electrodes, resulting in electrode surfaces smooth at the 1 μm level. By smoothly changing the electric potentials on the control-electrode segments, we were able to translate our trapping potential and move ions between two locations (traps #2 and #4 in Fig. 2).

Details of the experiments can be found in Ref. [20]. The key results were as follows:

(1) **Adiabatic transfer:** A single ion could be transferred between traps #2 and #4, a distance of 1.2 mm, in 25 μs while being kept in its ground state of motion. This time is approximately equal to the logic gate time, so if the transfer can be made somewhat faster in future work, the transfer time need not add a significant overhead

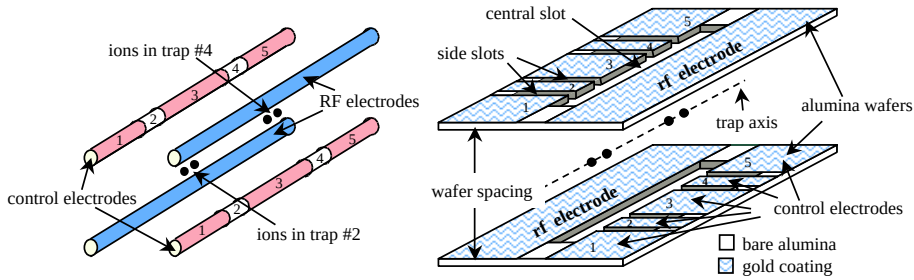

Figure 2: The "dual" linear ion trap (drawings not to scale). The left side of the diagram shows the idealized four-rod geometry; the right side shows the wafer-stack implementation. The two trap wafers are spaced with two 360 μm thick alumina pieces (not shown) that are placed between them along the short edges. The pairs of control electrodes are numbered 1 through 5 for reference. The two trap locations, #2 and #4, shown in the figure are labeled by the electrode on which they are centered. The axial length of electrode 1 (2,3,4,5) is 1100 μm (400 μm, 800 μm, 400 μm, 1100 μm). For 8.0 V applied to electrodes 1, 3, and 5 and 0.0 V applied to electrodes 2 and 4 the axial trap frequency in each trap was 2.9 MHz for a single $^9Be^+$ ion. The peak amplitude of the applied RF voltage was about 500 V. The RF drive frequency was 230 MHz.

in computation time.
(2) **Spin coherence:** By performing a two-zone Ramsey experiment with the two zones located at traps #2 and #4, we could show that no spin coherence was lost during transfer (to within our measurement precision of 0.5 %).
(3) **Robustness:** No ion loss was observed during transfer (in any set of experiments, $> 10^6$ transfers was typical).
(4) **Ion "splitting":** After placing two ions in a trap centered on electrodes #3, by increasing the potential on these electrodes, a potential wedge was inserted between the ions, separating them into traps #2 and #4. The separation was accomplished with $\simeq$ 95 % efficiency in a time of several milliseconds and the ions in their final respective wells had heated significantly ($\langle n \rangle \simeq 150$).

The heating that was observed upon separating ions was anticipated; to combat it, we expect that some sort of sympathetic re-cooling must be employed [6]. In the context of quantum computing, sympathetic cooling has been reported for like species (Ca^+) [35] and on isotopes of Cd^+ [36]. Recently we have sympathetically cooled $^9Be^+$ ions by Doppler cooling simultaneously trapped Mg^+ ions. On the other hand, we believe the heating can be reduced and the separation time decreased substantially in future experiments. For example, the geometry of this dual trap is not well-suited for separating ions. At the minimum center-of-mass axial trap frequency during separation ($\sim$ 90 kHz) the ions are separated by about 50 μm. Yet, in the experiments reported here, we effectively insert an approximately 800 μm wide potential wedge between them at this point, making separation very sensitive to small field offsets. If we employ electrode dimensions where the distance from the ion to the nearest control electrode is about 50 μm, this should allow us to make the width of wedge (electrode #3 in Fig. 2) approximately equal to this distance and make electrode voltage control much less stringent. Current efforts are therefore devoted to constructing smaller

trap structures while maintaining high-quality electrode surfaces in order to suppress heating [20].

4.2 Perspective

The obstacles to building a large-scale quantum computer appear to be technical rather than fundamental. However, by anyone's reckoning, realizing such a device will be extremely difficult and take a long time. Therefore, it is important to establish some intermediate goals upon which projections about scaling can be made. A couple of the more important interim goals appear to be:
(1) Error correction [37]. Here, a superposition state of a physical spin qubit is encoded into a "logical" qubit composed of several entangled physical qubits. Measurements of a subset of these bits allows one to correct for phase or bit-flip errors on any of the physical qubits. By repeating the encoding and measurement process, the logical bit can be preserved while under the influence of decoherence.[4]
(2) High-fidelity logic operations. The probability of an error generated by logic operations must be less than 10^{-4} or smaller [29] in order for error correction to enable arbitrarily long computations. For example, laser beam intensity stability is crucial; also, spontaneous emission can be an important limitation [38]. For the case of stimulated-Raman transitions, we desire a large ratio of fine-structure splitting to excited-state lifetime to suppress spontaneous emission. This rules out $^9Be^+$ as the ultimate qubit and favors ions such as Sr^+, Cd^+ [36], or Hg^+ [39].

5 Fundamental tests, measurement applications

The ability to coherently manipulate entangled quantum states, at least on a small scale, has enabled some demonstrations and tests of quantum mechanical principles that would otherwise remain as gedanken experiments. For trapped ions, nonclassical motional states have been engineered by use of the basic elements of quantum logic [8] and their properties determined through tomographic methods [40]. Motional Schrödinger-cat states have been generated [25] and the scaling of their decoherence based on the size of the cat state has been verified [26, 41]. A scheme for generation of arbitrary motional states has recently been demonstrated on a single ion [42]. Entanglement of up to four separate ions has been generated deterministically ("on demand") [18, 43] without the need for post-selection as in experiments using parametric down-conversion of photons. This enabled the first experiment showing a violation of Bell's inequalities (on massive particles) while defeating the "detection loophole" [44]. Treated as a small quantum processor, the trapped ion system can simulate the dynamics of other systems such as nonlinear optical beam splitters [45]. An exciting possibility is that these studies might eventually uncover some as-yet-unseen fundamental source of decoherence (see, for example, Ref. [46]).

A goal of the NIST experiments has been to use entanglement ("spin-squeezing") to increase the signal-to-noise ratio in spectroscopy and atomic clocks [47, 48]. An experiment on two ions has recently shown such squeezing [49] and although not yet of practical use, we could show that the squeezing that was obtained led to a signal-

[4] Passive means of fighting decoherence such as decoherence-free-subspaces have recently been demonstrated for ions [19] and might also be employed directly in future quantum computation [34].

to-noise ratio higher than could possibly be attained without entanglement. Simple quantum processing might also be used to aid in quantum measurement readout with potential applications to mass spectroscopy [50] and frequency standards [51].

6 Acknowledgements

We thank S. Bize, M. Jensen, and D. Smith for helpful comments on the manuscript. This work was supported by the U. S. National Security Agency (NSA) and Advanced Research and Development Activity (ARDA) under Contract No. MOD-7171.00, the U. S. Office of Naval Research (ONR), and the U. S. National Reconnaissance Office (NRO). The article is a contribution of NIST and not subject to U.S. copyright.

References

[1] J. I. Cirac and P. Zoller, Phys. Rev. Lett. **74**, 4091 (1995).

[2] D. Jaksch *et al.*, Phys. Rev. Lett. **85**, 2208 (2000).

[3] D. P. DiVincenzo, Phys. Rev. A **51**, 1015 (1995).

[4] A. Barenco *et al.*, Phys. Rev. A **52**, 3457 (1995).

[5] D. P. DiVincenzo, in *Scalable Quantum Computers*, edited by S. L. Braunstein and H. K. Lo (Wiley-VCH, Berlin, 2001), pp. 1–13.

[6] D. J. Wineland *et al.*, J. Res. Nat. Inst. Stand. Tech. **103**, 259 (1998).

[7] J. M. Raimond, M. Brune, and S. Haroche, Rev. Mod. Phys. **73**, 565 (2001).

[8] D. M. Meekhof *et al.*, Phys. Rev. Lett. **76**, 1796 (1996).

[9] C. Roos *et al.*, Phys. Rev. Lett. **83**, 4713 (1999).

[10] F. Diedrich *et al.*, Phys. Rev. Lett. **62**, 403 (1989).

[11] C. Monroe *et al.*, Phys. Rev. Lett. **75**, (1995).

[12] C. F. Roos *et al.*, Phys. Rev. Lett. **85**, 5547 (2000).

[13] R. Blatt and P. Zoller, Eur. J. Phys. **9**, 250 (1988).

[14] C. Monroe *et al.*, Phys. Rev. Lett. **75**, 4714 (1995).

[15] A. Sørensen and K. Mølmer, Phys. Rev. Lett. **82**, 1971 (1999).

[16] A. Sørensen and K. Mølmer, Phys. Rev. A **62**, 02231 (2000).

[17] E. Solano, R. L. de Matos Filho, and N. Zagury, Phys. Rev. A **59**, 2539 (1999).

[18] C. A. Sackett *et al.*, Nature **404**, 256 (2000).

[19] D. Kielpinski *et al.*, Science **291**, 1013 (2001).

[20] M. A. Rowe *et al.*, Quant. Inform. Comp. **2**, 257 (2002).

[21] B. DeMarco *et al.*, submitted for publication .

[22] C. Monroe *et al.*, Phys. Rev. A **55**, R2489 (1997).

[23] D. Leibfried *et al.*, in preparation .

[24] D. F. Walls and G. J. Milburn, *Quantum Optics*, 1st ed. (Springer, Berlin, 1994).

[25] C. Monroe, D. M. Meekhof, B. E. King, and D. J. Wineland, Science **272**, 1131 (1996).

[26] C. J. Myatt *et al.*, Nature **403**, 269 (2000).

[27] G. J. Milburn, S. Schneider, and D. F. James, in *Scalable Quantum Computers*, edited by S. L. Braunstein, H. K. Lo, and P. Kok (Wiley-VCH, Berlin, 2000), pp. 31–40.

[28] X. Wang, A. Sørensen, and K. Mølmer, Phys. Rev. Lett. **86**, 3907 (2001).

[29] A. M. Steane and D. M. Lucas, in *Scalable Quantum Computers*, edited by S. L. Braunstein, H. K. Lo, and P. Kok (Wiley-VCH, Berlin, 2000), pp. 69–88.

[30] J. I. Cirac, P. Zoller, H. J. Kimble, and H. Mabuchi, Phys. Rev. Lett. **78**, 3221 (1997).

[31] T. Pellizzari, Phys. Rev. Lett. **79**, 5242 (1997).

[32] R. G. DeVoe, Phys. Rev. A **58**, 910 (1998).

[33] J. I. Cirac and P. Zoller, Nature **404**, 579 (2000).

[34] D. Kielpinski, C. Monroe, and D. J. Wineland, Nature **417**, 709 (2002).

[35] H. Rohde *et al.*, J. Opt. B: Quantum Semiclass. Opt. **3**, S34 (2001).

[36] B. B. Blinov *et al.*, Phys. Rev. A **65**, 040304 (2002).

[37] M. A. Nielsen and I. L. Chuang, *Quantum Computation and Quantum Information*, 1st ed. (Cambridge Univ. Press, Cambridge, 2000).

[38] M. B. Plenio and P. L. Knight, Proc. R. Soc. Lond. A **453**, 2017 (1997).

[39] D. J. Wineland, Proc. Fermi School on Quantum Computation, Nuovo Cimento, to be published .

[40] D. Leibfried *et al.*, Phys. Rev. Lett. **77**, 4281 (1996).

[41] Q. A. Turchette *et al.*, Phys. Rev. A **62**, 053807 (2000).

[42] A. Ben-Kish *et al.*, submitted for publication .

[43] Q. A. Turchette *et al.*, Phys. Rev. Lett. **81**, 1525 (1998).

[44] M. A. Rowe *et al.*, Nature **409**, 791 (2001).

[45] D. Leibfried *et al.*, submitted for publication .

[46] A. J. Leggett, Physics World **12**, 73 (1999).

[47] D. J. Wineland *et al.*, Phys. Rev. A **46**, R6797 (1992).

[48] J. J. Bollinger, W. M. Itano, D. J. Wineland, and D. J. Heinzen, Phys. Rev. A **54**, R4649 (1996).

[49] V. Meyer *et al.*, Phys. Rev. Lett. **86**, 5870 (2001).

[50] D. J. Heinzen and D. J. Wineland, Phys. Rev. A **42**, 2977 (1990).

[51] D. J. Wineland *et al.*, in *Proc. 6th Symposium Frequency Standards and Metrology*, edited by P. Gill (World Scientific, Singapore, 2002), pp. 361–368.